Journal of Bioscience and Bioengineering
VOL. 128 No. 1, 103–109, 2019

www.elsevier.com/locate/jbiosc

Harvesting of *Scenedesmus acuminatus* using ultrafiltration membranes operated in alternative feed directions

Li Yang,[1,2] Lan Wang,[1,2] Sumeng Ren,[1,2] Bo Pan,[1,2] Jing Li,[1,2] Xuezhi Zhang,[1,2,*] Yongsheng Chen,[1,2,3] and Qiang Hu[1,2,4,5]

Center for Microalgal Biotechnology and Biofuels, Institute of Hydrobiology, Chinese Academy of Sciences, Wuhan 430072, China,[1] Key Laboratory for Algal Biology, Institute of Hydrobiology, Chinese Academy of Sciences, Wuhan, Hubei 430072, China,[2] School of Civil and Environmental Engineering, Georgia Institute of Technology, Atlanta, GA 30332, USA,[3] Microalgae Biotechnology Center, China Electronics Engineering Design Institute, State Development & Investment Corporation, Beijing 100142, China,[4] and Beijing Key Laboratory of Algae Biomass, Beijing 100142, China[5]

Received 29 May 2018; accepted 13 January 2019
Available online 18 February 2019

Ultrafiltration membrane harvesting of *Scenedesmus acuminatus* was tested using alternative feed (AF) directions, i.e., bottom feed-top feed cycle and traditional bottom feed (BF). Both operations were investigated to compare the membrane performance and membrane fouling in microalgal harvesting process by scanning electron microscope (SEM), confocal laser scanning microscopy (CLSM) and Fourier transform infrared (FTIR). The results showed that when the AF was used with and without backwashing, average flux increased by 27.9% and 17.9%, respectively, comparing with BF (68 L m^{-2} h^{-1}) and the final dry weight reached 197 g L^{-1} and 175.8 g L^{-1}, respectively. Microalgal cell deposition on AF membrane was reduced from 1.44 × 10^5 cell cm^{-2} on BF membrane to 7.12 × 10^4 cell cm^{-2} on AF membrane, according to SEM observation. The protein and polysaccharides on the AF membrane surface were also reduced according to CLSM and FTIR analysis. Fouling analysis along the fiber length revealed that fouling was most severe at the top section for BF as a result of a lower shear rate at the outlet. AF operation generated dynamic filtration by frequently switching flow directions, increasing the shear rate at both the top and bottom of the fibers, and therefore filtration and clean process simultaneously provided good performance.

[**Key words:** Microalgal harvesting; Alternative feed; Flux; Fouling; Dynamic filtration]

Microalgal biotechnology has been recognized as a promising solution for bioproducts, biofuel and bioremediation (1–4). However, microalgal biomass harvesting still remains one of the bottlenecks for cell-water separation as the typical unicellular cells are as small as 2–30 μm (5), with a density similar to water, and most importantly, they are in a huge volume of water that must be processed. As a nonchemical-based harvesting process, membrane harvesting has been increasingly used in biomass recovering and culture media recycling (6–10). During the microalgal harvesting process, membrane fouling by microalgal cells and organic matter in the media greatly reduces membrane flux and harvesting efficiency (11).

Hollow fiber membranes are used to harvest microalga under the cross-flow mode. Microalgal suspension is pumped into the membrane fibers from the bottom and the retentate leaves the fiber from the top, while permeate is driven through the membrane pores into the fiber wall under the pressure difference. As the filtration continues, microalgal cake layers pile up and become thicker and thicker. At the same time pores are blocked or stained by microalgal cells, cell debris and/or organic matter depending on the cellular mass size or properties (12,13). Meanwhile, the microalgal biomass concentration becomes higher and higher, i.e., 50–100 g L^{-1} (14), which is typically 200 times higher than the total suspended solid concentration in the municipal wastewater treatment process, which is about 200 mg L^{-1}. The high solid content, as well as the algogenic organic matter (AOM) loading is a tremendous challenge for continuing the harvesting process (15).

Increasing cross-flow velocity generates higher shear forces across the membrane surface and increases the average flux (16,17). However, the energy consumption needed to maintain the high cross-flow velocity is not affordable for microalgal harvesting. Some researchers have presented dynamic filtration, which induces constant changes in shear force or feed flow patterns, using vibrating membranes (18–20) or dynamic disk filtration (21,22). For example, dynamic ultrafiltration membranes with axial vibration are able to effectively mitigate membrane fouling during filtration, and make it difficult to form a compact algae cake layer at frequency of 10 Hz and amplitude of 1 cm (23). However, these traditional dynamic filtrations not only increased the cost of the device, but added the tremendous operational energy. Most importantly, these methods are difficult to scale up.

Alternative feed (AF) is novel dynamic filtration with switching feed flow direction across the membrane surface, and thus the feed direction changed frequently. As a result both the top and bottom positions of the fiber were flushed fully, and the higher flux was

* Corresponding author at: Center for Microalgal Biotechnology and Biofuels, Institute of Hydrobiology, Chinese Academy of Sciences, Wuhan 430072, China. Tel.: +86 27 6878 0929; fax: +86 27 6878 0917.
E-mail address: zhangxuezhi@ihb.ac.cn (X. Zhang).

1389-1723/$ – see front matter
https://doi.org/10.1016/j.jbiosc.2019.01.007

maintained. Due to these advantages, AF has been increasingly used in reverse osmosis desalination process in order to prevent scale crystal formation on the membrane surface (24,25), and mitigate the membrane fouling and concentration polarization (26). However, there is limited study on the mechanism of membrane fouling alleviation, as well as operation parameters optimization and membrane fouling characterization.

Along the membrane length there is a rapid drop in pressure and velocity, and thus flux also drops rapidly as cake layer piles up. The problem is complicated by the fact that a low pressure at the outlet reduces the efficiency of the outlet section of the membrane module, on the other hand low velocity at the outlet induces insufficient scour and fouling layer forming on the membrane surface. In this study, microalgal harvesting with membranes operating under AF was tested. The objectives of this study were: (i) to test the hypothesis that membrane fouling varies along the fiber length, and the fouling near the end of the bottom feed (BF) operated membrane fibers is more severe as a result of the decreased shearing rate, and (ii) dynamic filtration by alternating feed direction alleviates microalgal fouling to achieve higher membrane flux.

MATERIALS AND METHODS

Microalga cultivation and membrane unit operated using alternative feed directions The green microalga, *Scenedesmus acuminatus* (GT-2) are obtained from Microalgae Biotechnology Center at State Development and Investment Co. (SDIC), China, which is selected as a model strain because it is ubiquitous in the water environment and is often selected for microalga-based wastewater treatment and for production of biofuels (27–31). Fresh microalgal suspensions were cultured in 15 L flat panel photobioreactors with a BG11 culture media. The pH of the culture media was 7.1–8.5. The average temperature was 25°C, and the maximum solar irradiation was 250 μmol m^{-2} s^{-1}. The morphology of the *S. acuminatus* cells was observed under light microscopy and the dry weight was measured daily.

PVC hollow fiber ultrafiltration membrane modules with a filtration area of 0.13 m^2 and molecular weight cut off (MWCO) of 50 kDa (Litree Co., Hainan, China) were used for the microalgal harvesting. The membrane was hydrophilic with a water contact angle of 67 ± 2°. The modules were 0.25 m in length, and the inner and outer diameters of the fiber were 1.0 mm and 1.66 mm, respectively.

The membrane harvesting experiments were carried out by a membrane unit specially designed to be operated in the alternative feed directions. The operation schematic diagram of AF filtration is shown in Fig. 1. Unlike the traditional BF flow operation in which the feed was pumped into the membrane module through the bottom, in the AF operation, the module was bottom feed first then switched to top feed after a certain interval. The alternation of feed direction continued until the harvesting was finished. The permeate weight was recorded every second by a balance and transmitted into a computer for flux calculation.

Harvesting of *S. acuminatus* using ultrafiltration operated in alternative feed directions Before the experiment, flux was tested at different trans-membrane pressures (TMPs) using deionized water. During the membrane harvesting process, TMP was maintained at 34.5 kPa by a regulatory valve in the

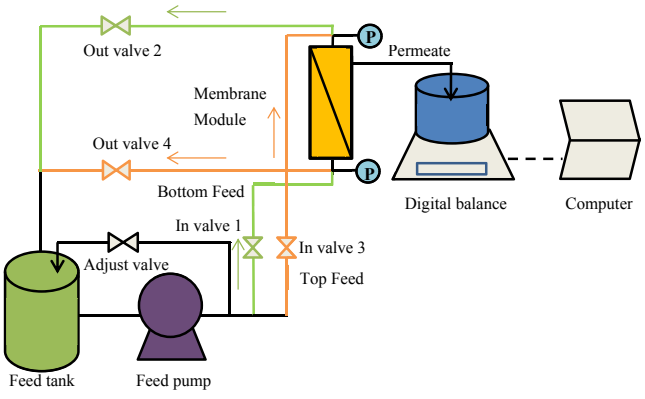

FIG. 1. Schematic diagram of membrane harvesting unit which can be operated in both alternative feed (AF) directions, and traditional bottom feed (BF) direction.

filtration system. After a certain interval, an air assisted backwashing method was adopted to recover the membrane flux (14).

Firstly, influence of backwashing intervals on the flux of BF operation were compared at different intervals of 10, 15, 30 and 60 min.

Backwashing interval is defined as the length of one filtration period between subsequent backwashing (32). Then, the different frequencies of feed flow alternation (1.5, 3, 5, 7.5 and 15 min) were evaluated for AF, and the average flux was compared with BF filtration at the optimized backwashing interval. The influence of different cross-flow velocities on the performance of AF was further evaluated at cross-flow velocities of 0.1, 0.2 and 0.3 m s^{-1} by adjusting the control valve and the out valve. The average flux and instantaneous flux were compared to get the optimal velocity.

After each harvesting, the membrane was physically cleaned with deionized water, followed by a chemical cleaning with 400 ppm NaClO for two hours trans-membrane circulation. Flux recovery after physical cleaning and chemical cleaning were calculated.

The optimized parameters of AF were applied for the harvesting of 20 L *S. acuminatus* suspension at an initial dry weight of 2.0 g L^{-1}. The frequency of flow direction was switched every 3 min. The membranes were backwashed every 15 min for flux recovery. AF with flow direction switches every 3 min without backwashing was also evaluated. The results of AF operations were then compared with the traditional bottom feed flow which received backwashing every 15 min. The flux throughout the harvesting process was recorded, and the flux declining rate ($D(n)$) and flux recovery ($R(n)$) were calculated using Eqs. 1 and 2, respectively (14,33).

$$D(n) = \frac{J_0 - J_{i.15}}{J_0} \tag{1}$$

$$R(n) = \frac{J_{i+1.1}}{J_0} \tag{2}$$

where J_0 (L m^{-2} h^{-1}) is water flux, $J_{i.15}$ (L m^{-2} h^{-1}) is instantaneous flux at 15 min for cycle n and $J_{i+1.1}$ (L m^{-2} h^{-1}) is instantaneous flux at 1 min of cycle i+1 (Fig. S3).

The average flux (J_a, L m^{-2} h^{-1}) was calculated using Eq. 3:

$$J_a = \frac{\sum_{i=1}^{n}\sum_{j=1}^{15} J_{i,j} \times t}{\sum_{i=1}^{n}\sum_{j=1}^{15} t} \tag{3}$$

where i is the number of filtration cycle, j is the filtration time in each cycle, which is set from 1st min, 2nd min and 3rd min to 15th min, $J_{i,j}$ (L m^{-2} h^{-1}) is the instantaneous flux at j min of filtration cycle i, and t is the integration interval to calculate the average flux, which is set as 1 min in this study.

After each harvesting, the volumetric reduction factor (VRF) and concentration factor (CF) were calculated to evaluate the harvesting efficiency using the following equations:

$$\mathrm{VRF} = \frac{V_0}{V_f} \tag{4}$$

$$\mathrm{CF} = \frac{C_f}{C_0} \tag{5}$$

where V_0 is initial volume (L), V_f is final volume (L), C_f is final algal concentration (g L^{-1}), and C_0 is initial algal concentration (g L^{-1}).

The backwashing reversible resistance (R_r) and backwashing irreversible resistance (R_{ir}) were calculated to evaluate the performance of fouling alleviation, using fouling in series analysis reported by Zhang et al. (34) and Zhang et al. (35):

$$R_m = \frac{\Delta P}{\mu J_0} \tag{6}$$

$$R = \frac{\Delta P}{\mu J} \tag{7}$$

$$R_r = \frac{\Delta P}{\mu \Delta J} \tag{8}$$

$$R_{ir} = R - R_r - R_m \tag{9}$$

where R_m is membrane resistance (m^{-1}), ΔP is trans-membrane pressure (Pa), μ is viscosity of permeate (Pa s), J_0 is water flux (L m^{-2} h^{-1}), R is total resistance (m^{-1}), J is permeate flux (L m^{-2} h^{-1}), R_r is reversible resistance (m^{-1}), ΔJ is the difference in fluxes before and after backwashing (L m^{-2} h^{-1}) and R_{ir} is irreversible resistance (m^{-1}).

The unit energy consumption of BF and AF operation was calculated. The power of pump (P_p, kW) is calculated using the Eq. 10 available in the Engineering Tool Box (https://www.engineeringtoolbox.com/pumps-power-d_505.html):

$$P_p = \frac{q\rho gh}{3.6 \times 10^6 \eta} \tag{10}$$

where q is flow rate ($m^3\ h^{-1}$), ρ ($kg\ m^{-3}$) is density of microalgal suspension, g ($m\ s^{-2}$) is gravity, h (m) is differential head and η is the efficiency of the pump.

The power of air compressor (P_a, kW) consumed during the backwashing process of BF is calculated using Eq. 11 available in the Engineering Tool Box (https://www.engineeringtoolbox.com/horsepower-compressed-air-d_1363.html):

$$P_a = \frac{63NV_aP_1k\left[\left(\frac{P_2}{P_1}\right)^{\frac{k-1}{Nk}} - 1\right]}{33000(k-1)} \quad (11)$$

where N is number of compression stages, k is adiabatic expansion coefficient, P_1 (psi) is absolute initial atmospheric pressure, P_2 (psi) is absolute final atmospheric pressure, V_a ($m^3\ h^{-1}$) is volume of air at atmospheric pressure.

The unit energy consumption per m^3 (E) is calculated by Eq. 12:

$$E = \frac{Pt}{V_l} \quad (12)$$

where P (kW) is energy consumption for pump or air compressor, t (h) is running time, and V_l (m^{-3}) is the volume of harvested microalga.

Membrane fouling characterization The Hitachi S4800 cold cathode field-emission scanning electron microscope (FE-SEM from Hatchi America, Ltd., Tarrytown, NY, USA) was used to obtain the morphological information of the microalgal cells deposited on the inner surface of the membrane operated in the AF and BF mode with backwashing. Fouled membrane fibers in wet mode were broken with liquid nitrogen to obtain membrane fragments. Membrane samples were positioned on a metal holder, then sputter coated with gold under vacuum for 3 min. The scanning was performed at an accelerating voltage of 10 kV. Then the number of *S. acuminatus* cells on the SEM images were counted using Image J software method described in the literature (36,37). At least 20 images were analyzed to obtain the numbers of cells attached on the fouled membrane. The number of *S. acuminatus* cells on the SEM pictures as well as the membrane area were quantified using Image J. The numbers of cells per unit membrane filtration area is calculated using the following equation:

$$n = \frac{N_t}{s} \quad (13)$$

where n is cell number per area (number cm^{-2}), N_t is the total cell number on the picture and s is the area of the membrane (cm^2).

The Leica TCS SP8 laser confocal microscope (Leica Microsystems, Wetzlar, Germany) was used to characterize protein and polysaccharide fouling on the fouled membrane under the AF and BF operation with backwashing. Several membrane fragments were immersed in 0.1 M 1 mL $NaHCO_3$ buffer solution in EP tubes for 30 min to keep the amine group in non-protonated form. Then 10 μL fluorescein isothiocyanate (FITC) solution (10 $g\ L^{-1}$) was added into the EP tubes and incubated for 2 h in the dark. The membrane fragments were washed twice by phosphate buffered saline (PBS) to remove excess stain. The next step was to add 10 μL calcofluor white solution to the EP tubes, incubating for 30 min in the dark. Finally, the membrane fragments were washed twice again by PBS before laser confocal microscope observation.

An attenuated total reflectance-Fourier transform infrared (ATR-FTIR, Spectrum One, PerkinElmer, Waltham, MA, USA) was used to identify the functional group of foulants on the membrane's inner surface. Dry membranes under the AF and BF operation with backwashing were attached onto microscope slides and analyzed at 2 cm^{-1} intervals, and the spectrum was recorded at 4000-400 cm^{-1}.

Fouling analysis along the fiber length Membrane fouling differs along the membrane length (38). For research the mechanism of AF fouling membrane fouling level along the fiber length was tested. Membrane fouling along the fiber was analyzed by testing pure water flux of fibers taken from the membrane housing. After harvesting 20 L of microalgal suspension using the BF and AF methods, the membrane module was analyzed by an autopsy to determine the effects of different feed operations on the fouling along the fiber length. This consisted of removing the fibers from the membrane housing first. Every fiber was cut into three sections (i.e., the top, middle and bottom sections). These sections were then assembled into single fiber membrane modules, and three modules were assembled for each section. Pure water fluxes were tested for each module at a constant TMP of 6.8 kPa and cross velocity of 0.1 $m\ s^{-1}$ using the KR2i tangential flow filtration system (Spectrum Laboratories, Inc., Rancho Dominguez, CA, USA). The flux of the single membrane module and membrane module of 0.13 m^2 were uniform (data not shown). The average flux of the top, middle and bottom section of three single fibers modules was tested.

RESULTS AND DISCUSSION

Selection of optimal harvesting parameters Backwashing interval is the most important parameter, affecting the flux recovery both for AF and BF. Different backwashing intervals were first optimized for BF operation shown in Fig. 2A, varying from 10, 15, 30–60 min. It can be seen that flux declined as the filtration continued. The flux recovered more or less after each backwashing. As the backwashing interval decreased from 60 to 30 min, the average flux increased from 59.9 to 76.2 L $m^{-2}\ h^{-1}$, representing an approximate 27.2% increase. As the backwashing time interval reduced from 30 to 15 min, the average flux further increased from 76.2 to 84.3 L $m^{-2}\ h^{-1}$, increasing 10.5%. Meanwhile, the backwashing time interval further reduced from 15 min to 10 min, and flux reached a plateau of 84.6 L $m^{-2}\ h^{-1}$. The results indicate that the 15 min backwashing interval was the optimal value for the average flux, as more frequent backwashing did not result in a much higher flux increase, but it will increase operational cost and shorten membrane lifetime dramatically.

As shown in Fig. 2B, the flux declining over time during the harvesting of *S. acuminatus* at different alternative time of AF operation (1.5, 3, 7.5 and 15 min) with backwashing every 15 min, which was the optimized backwashing time interval for BF during testing. For comparison, the flux declining during BF operation was also tested with backwashing intervals of 15 min. The average flux of BF with 15 min backwashing interval was 96.3 L $m^{-2}\ h^{-1}$, and it decreased to 82.8 L $m^{-2}\ h^{-1}$ when AF was used with the alternative time of 15 min, which may be caused by the increasing of the flux reduction during top feed. The CFD simulation confirmed that there is flow turbulence in the top when the module is feed from the top (Fig. S4).

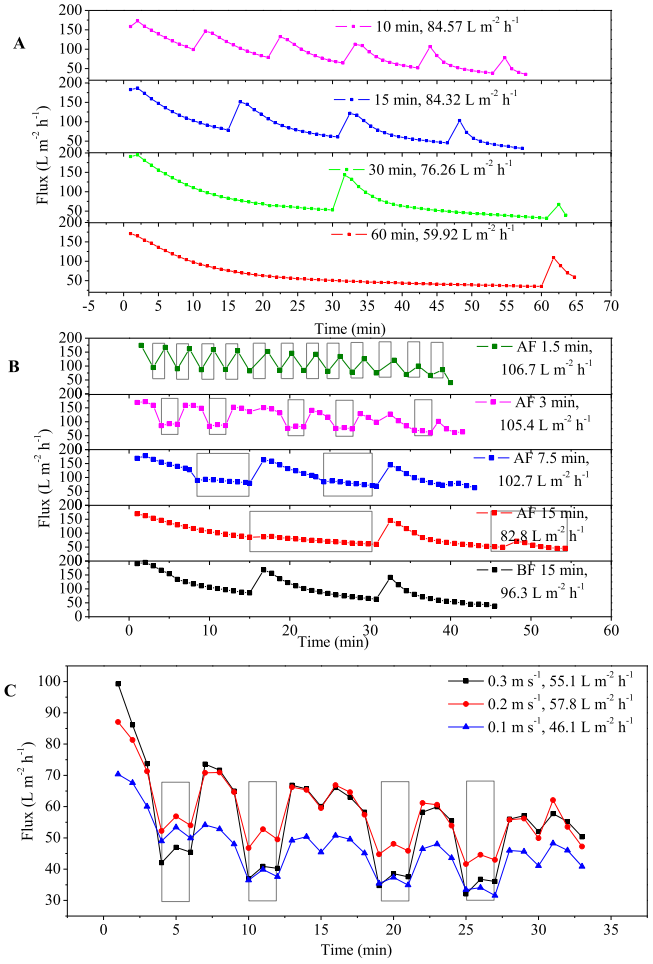

FIG. 2. (A) Flux declining over time at different backwash interval under bottom feed (BF) operation; (B) flux changes over time at different frequencies of feed direction alternation; (C) flux changes over time at different cross-flow velocity. The top feed period during the alternative feed (AF) operation was marked with gray boxes.

When alternative time reduced from 15 to 7.5 and then to 3 min, although the top feed still resulted in a lower flux than the bottom feed, the more frequent switching of flow direction helped to maintain a higher flux, and the average flux increased from 82.8 L m^{-2} h^{-1}–102.7 L m^{-2} h^{-1} and then to 105.4 L m^{-2} h^{-1}. Further shortening alternative time from 3 min to 1.5 min only increased the flux to 106.7 L m^{-2} h^{-1}. Thus a 3 min alternative time was selected as the optimized value.

The flux change over time of different cross-flow velocities is shown in Fig. 2C. The cross-flow velocities range from 0.1 to 0.3 m s^{-1} at a TMP of 34.5 kPa. When cross-flow velocities increased from 0.1 m s^{-1} to 0.2 m s^{-1} the average flux increased from 46.1 L m^{-2} h^{-1}–57.8 L m^{-2} h^{-1} increasing 25.2%, but the cross-flow velocities increase from 0.2 m s^{-1} to 0.3 m s^{-1}, and the average flux has no increase.

The flux of 0.1 m s^{-1} was always lower than flux of 0.3 and 0.2 m s^{-1} for both bottom feed and top feed. The flux of 0.3 m s^{-1} was almost the same as that of 0.2 m s^{-1} during the bottom feed, while it was much lower during the top feed, which may be due to the poor distribution. So the average flux of 0.3 m s^{-1} remains lower than the flux of 0.2 m s^{-1}. Lobo et al. (39) used tubular ceramic membranes and filtrated vegetable oil with anionic and non-ionic emulsifiers. They found that when cross-flow velocities increased and the pumping costs increased but the permeate flux did not improve significantly. So 0.2 m s^{-1} was chosen as the optimizing cross-flow velocity.

Harvesting of *S. acuminatus* using ultrafiltration operated in alternative feed directions After the optimization of alternative frequency and cross-flow velocity, AF operation was tested for the bench scale harvesting of 20 L *S. acuminatus* with flow direction switching every 3 min, and the cross-flow velocity was kept 0.2 m s^{-1} both with backwashing intervals of 15 min and without backwashing. In comparison, the changes in flux of the BF operation with backwashing interval of 15 min were also presented. Changes in flux under three different operation modes are shown in Fig. 3A.

For BF, flux dropped in the first filtration cycle from 174.6 L m^{-2} h^{-1}–71.4 L m^{-2} h^{-1}. Then 86.7% flux was recovered, reaching 151.0 L m^{-2} h^{-1} after backwashing and then dropped again to 67.1 L m^{-2} h^{-1}. The flux declining-recovery-declining cycle was repeated continually until the harvesting process was finished. The average flux was only 68 L m^{-2} h^{-1} due to the rapid drop during each filtration cycle.

Alternative flow without backwashing is the mode that the bottom feed and top feed processes were used as an alternative every 3 min and there was no backwashing during the whole harvesting process. As can be seen in Fig. 3A, top feed stopped the declining of the flux, while the subsequent bottom feed increased the flux significantly. The average flux of AF without backwashing was 80.0 L m^{-2} h^{-1}, which increased 17.9%, compared with BF. Unit energy consumption of AF operation is 0.13 kWh m^{-3} and BF operation with backwashing is 0.24 kWh m^{-3} for one harvesting process. The results suggested that energy consumption of AF operation without backwashing is 45.8% lower than BF operation with backwashing (Tables S2 and S3).

During the harvesting of *S. acuminatus* using AF directions with backwashing, the bottom feed and top feed was alternatively used every 3 min, and every 15 min the module was backwashed. After the backwashing the AF operation re-stated with the bottom feed first. After the first 15 min filtration cycle, the flux started to drop from 185.9 L m^{-2} h^{-1}–117.3 L m^{-2} h^{-1}. Then backwashing recovered the flux to as high as 157.6 L m^{-2} h^{-1}. Simultaneously, because of backwashing, for every backwashing 50 mL of permeate used for rinsing the membrane pore came back to the feed tank for repeat filtration. Therefore, although backwashing was shown to improve

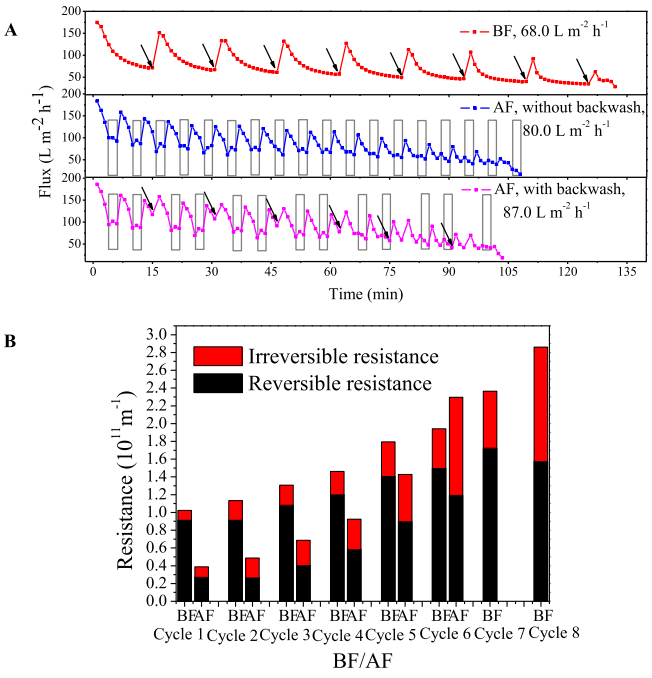

FIG. 3. (A) Changes in permeate flux during bench scale harvesting of *S. acuminatus* using bottom feed (BF) with backwashing, alternative feed (AF) without backwashing and with backwashing (backwashing events are labeled with arrows); (B) Changes in irreversible and reversible resistances during the harvesting process of BF and AF membrane both with backwashing.

flux recovery, more volume of feed needs to be handled, which is drawback of the applying of the backwashing. Nonetheless, the highest average flux of 87.0 L m^{-2} h^{-1} was achieved, which was represented a 27.9% increase above the average flux obtained in BF.

Filtration resistance analysis is often used for manifestation membrane fouling, which causes flux to decline and also affects flux recovery (40). Calculated flux decline rate and recovery proved that the decline rate of BF is higher than AF and the flux recovery of BF is lower than AF. The results of the reversible and irreversible resistance caused by backwashing during each BF and AF with backwashing filtration cycle are presented in Fig. 3B.

As the concentration preceding the reversible and irreversible resistances increase, the total resistance (total height of the column) and reversible resistance of BF was higher than that of AF throughout the harvesting, indicating that membranes in the BF mode fouled more severely than membrane in the AF mode. The irreversible resistance was not consistent with either the total resistance or reversible resistance, especially in the latter period.

In the AF mode the alternation of feed direction provided enough shear force to scour the foulants off the membrane surface, resulting in a cleaner membrane surface. So microalgal cake forming on the membrane is quite thin, and a lower reversible resistance is evident, but there is also an increased risk of contact between the algae-associated algogenic organic matter (AOM) and causing irreversible fouling (41). However, the portion of irreversible resistance is not a dominant concern since it is much less than the problems caused by reversible resistance. In the latter period, the microalga is so deeply condensed that the increased resistance is clearly visible, but it does not exceed the final two cycles of BF.

The VRF and CF of membrane harvesting using BF, AF without backwashing, and AF with backwashing were calculated and the results are shown in Table 1. The final dry weight after membrane harvesting by BF was 162.5 g L^{-1}, and the volume was reduced about to 0.11 L. The values of CF and VRF after membrane harvesting

TABLE 1. Comparison of concentration factor between BF and AF.

Flow direction	BF	AF (without backwashing)	AF (with backwashing)
Condensed dry weight ($g\ L^{-1}$)	162.5	175.8	197
VRF	190	200	250
CF	147.7	159.8	179.1
Average flux ($L\ m^{-2}\ h^{-1}$)	68	80	87
Condensed time (min)	132	108	103.5

by BF were 147.7 and 190, respectively. When AF was used without backwashing, the final dry weight increased to 175.8 g L^{-1}, and the CF and VRF reached 159.8 and 200, respectively, suggesting the AF was very efficient in microalgal harvesting in terms of both volume reduction and dry weight concentration. The backwashing process enhanced the performance even more. When AF operation was used, and the membrane was backwashed every 15 min, the final concentration reached 197 g L^{-1}, and the CF and VRF reached 179.1 and 250, respectively.

Monte et al. (42) harvested of *Dunaliella salina* by ultrafiltration allowed reaching a final concentration factor of 5.9, with an average permeate flux of 31 L m^{-2} h^{-1}. Zhang et al. (14) harvested *Scenedesmus quadricauda*, and the final dry weight reached a high value of 150.0 g L^{-1}; however, it takes 6 h to finish the bench scale harvesting of 20 L of microalgal suspension, and the average flux was 35.0 L m^{-2} h^{-1}. In this study, the AF increased the efficiency dramatically, and the final dry weight was 197 g L^{-1}, with an average flux of 87 L m^{-2} h^{-1}, representing 200% increase due to the efficient fouling control of AF.

Characterization of membrane fouling SEM images of fouled membranes under AF and BF operation are investigated (Fig. S1). The number of microalga on the AF membrane was almost half of those on the BF membrane, which was found 7.12×10^4 cell cm^{-2} and 1.44×10^5 cell cm^{-2} for AF and BF, respectively. Furthermore, most of the cells are aggregated on the BF membrane, but all the microalga were single cells on the AF membrane, indicating that the fouling of the AF membrane surface by microalgal cells was well controlled, resulting a higher average flux.

Confocal laser scanning microscopy (CLSM) analysis was conducted to observe the morphology of organic fouling on the membrane operated in the AF and BF modes, and the results are shown in Fig. 4. The green dots in the images indicate the presence of protein, and the blue light points indicate the presence of polysaccharide (43). The wide range of blue and green fluorescence in

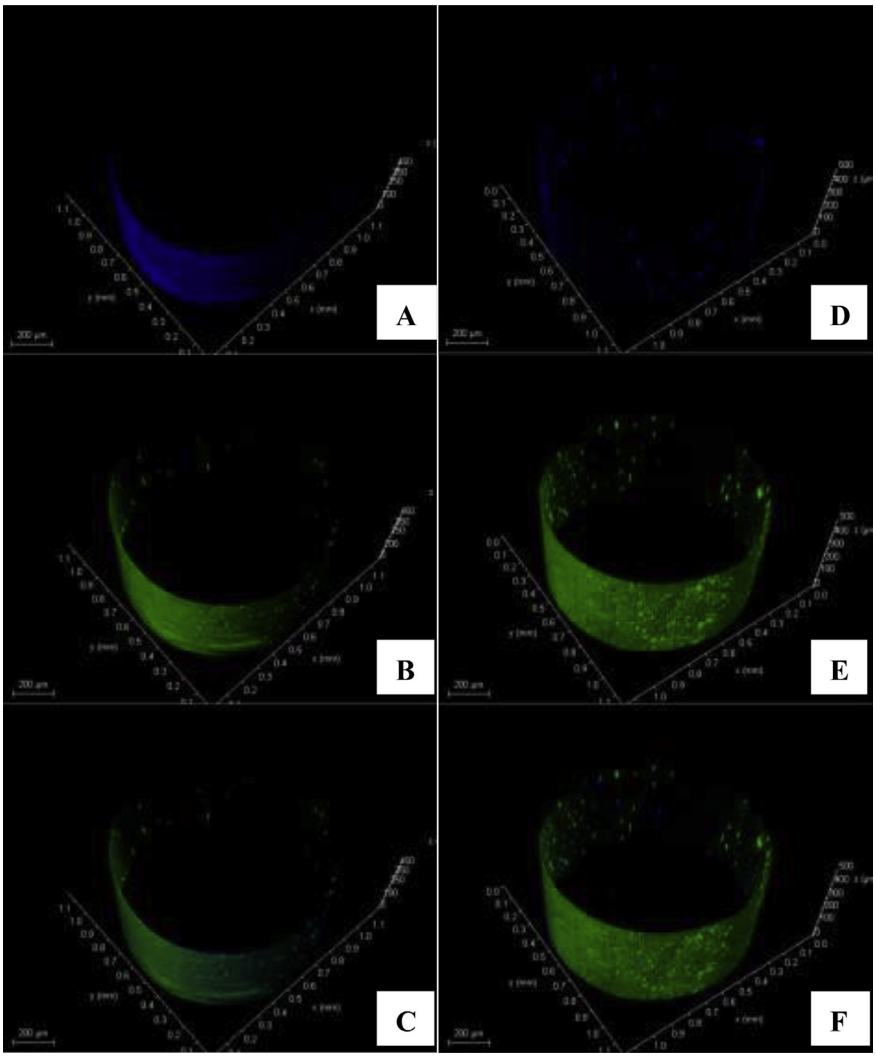

FIG. 4. CLSM images of alternative feed (AF) and bottom feed (BF) operated fouled membranes. AF operated membranes are shown in the left column as (A) polysaccharide, (B) protein, and (C) polysaccharide-protein fluorescence. BF operated membranes are shown in the right column as (D) polysaccharide, (E) protein, and (F) polysaccharide-protein fluorescence. Scale bar: 200 um.

TABLE 2. Flux distribution along the top, middle and bottom segments of membrane fibers used in AF operation, top and bottom feed.

Operation	Top (L m^{-2} h^{-1})	Middle (L m^{-2} h^{-1})	Bottom (L m^{-2} h^{-1})
BF (bottom feed)	2.4	11.5	11.1
Top feed	9.3	5.6	5.1
AF	9.8	12.0	8.1

the background is the residual dye on the membrane. Comparing the images, both the proteins and polysaccharides on the AF membrane surface were much fewer than those on the BF membrane, indicating that the amount of organic fouling of the AF membranes was greatly reduced. These results agree with the FTIR results. To explore the organic fouling on the membrane surface, FTIR was applied to scan the surface of BF, AF, and the virgin membrane (Fig. S2). Comparing foulants on both the AF and BF membranes, we found a large number of proteins on both two types of membranes (44). However, no carbohydrates were found on the AF membrane, so proteins rather than carbohydrates were determined to be the major contributor to fouling. Wu et al. (45) also found that membrane fouling was more likely to be caused by proteins rather than carbohydrates.

In the AF operation, the feed flow direction alternated every 3 min, which not only maintained the higher shear rates on the top or bottom parts of the fibers alternatively, but generated the dynamic shear across the membrane surface due to the frequent switching of flow direction. The dynamic shearing force across the membrane surface not only removed microalgal cell deposition, but also cleaned the organic foulants represented by proteins and polysaccharide from the membrane surface. This can help maintain the high flux during the harvesting of *S. acuminatus*.

Fouling analysis along the fiber length To understand why AF can help maintain high flux, the pure water flux of single fiber membranes in the top, middle and bottom positions of AF membrane were tested. As a comparison, pure water flux of fibers at the top, middle and bottom position were also tested under bottom feed and top feed conditions. The pure water flux is presented in Table 2. As shown in this table the flux is much lower than those in the former figures because this flux was tested at a cross-flow velocity of 0.1 m s^{-1} and a TMP of 6.8 kPa.

As shown in Table 2 for BF, the flux of the bottom segment was 11.1 L m^{-2} h^{-1}, with a resistance of 2.1 $\times$ 10^{12} m^{-1} (Table S1) and the flux of the top position was only 2.4 L m^{-2} h^{-1} with a resistance of 9.7 $\times$ 10^{12} m^{-1}, indicating the fouling on the top segment was much more severe. When membranes were used with top feed, the bottom flux was only 5.1 L m^{-2} h^{-1} and the top position flux was 9.3 L m^{-2} h^{-1}, and their resistance were 4.6 $\times$ 10^{12} m^{-1}, 2.5 $\times$ 10^{12} m^{-1}, respectively, indicating that the bottom segment fouling was much more severe. However, when membranes were used in AF, the middle position flux was the highest with a value of 12.1 L m^{-2} h^{-1}, with lowest resistance of 1.9 $\times$ 10^{12} m^{-1}, and the flux differences between top-middle and bottom-middle segments were much less than those of top feed and bottom feed, suggesting that fouling along the fibers was well alleviated through AF operation.

In the BF filtration, the cross velocity in the feed position was the largest and as the height increased, the cross velocity gradually decreased. The velocity of the feed was calculated at 0.22 m s^{-1} in the bottom but was reduced into 0.18 m s^{-1} at the top outlet, assuming the velocity is in linear decline based on the vertical position. The lower the cross velocity the weaker the scour is. So the foulants accumulated on the top position of the membrane resulted in a low flux (46,47). In AF, the feed direction changed frequently, so both the top and bottom positions of the fiber were flushed fully, and the higher flux was maintained.

Supplementary data to this article can be found online at https://doi.org/10.1016/j.jbiosc.2019.01.007.

ACKNOWLEDGMENTS

The authors gratefully appreciate the financial support from the National Natural Science Foundation of China (Grant 31672625 and 51678561). This work was also supported the One-Hundred Scholars Award from the Chinese Academy of Sciences (Y62305-1-Z01). The technical assistance from Juan Xu on CLSM analysis is gratefully acknowledged.

References

1. **Hu, Q., Sommerfeld, M., Jarvis, E., Ghirardi, M., Posewitz, M., Seibert, M., and Darzins, A.:** Microalgal triacylglycerols as feedstocks for biofuel production: perspectives and advances, Plant J., **54**, 621–639 (2008).
2. **Demirbas, A. and Fatih Demirbas, M.:** Importance of algae oil as a source of biodiesel, Energy Convers. Manage., **52**, 163–170 (2011).
3. **Zhu, L. D. and Hiltunen, E.:** Application of livestock waste compost to cultivate microalgae for bioproducts production: a feasible framework, Renew. Sustain. Energy Rev., **54**, 1285–1290 (2016).
4. **De Gouvion Saint Cyr, D., Wisniewski, C., Schrive, L., Farhi, E., and Rivasseau, C.:** Feasibility study of microfiltration for algae separation in an innovative nuclear effluents decontamination process, Sep. Purif. Technol., **125**, 126–135 (2014).
5. **Henderson, R., Parsons, S. A., and Jefferson, B.:** The impact of algal properties and pre-oxidation on solid-liquid separation of algae, Water Res., **42**, 1827–1845 (2008).
6. **Kim, D. G., La, H. J., Ahn, C. Y., Park, Y. H., and Oh, H. M.:** Harvest of *Scenedesmus* sp. with bioflocculant and reuse of culture medium for subsequent high-density cultures, Bioresour. Technol., **102**, 3163–3168 (2011).
7. **Sabia, A., Baldisserotto, C., Biondi, S., Marchesini, R., Tedeschi, P., Maietti, A., Giovanardi, M., Ferroni, L., and Pancaldi, S.:** Re-cultivation of *Neochloris oleoabundans* in exhausted autotrophic and mixotrophic media: the potential role of polyamines and free fatty acids, Appl. Microbiol. Biotechnol., **99**, 10597–10609 (2015).
8. **Hadj-Romdhane, F., Zheng, X., Jaouen, P., Pruvost, J., Grizeau, D., Croue, J. P., and Bourseau, P.:** 7-The culture of *Chlorella vulgaris* in a recycled supernatant: effects on biomass production and medium quality, Bioresour. Technol., **132**, 285–292 (2013).
9. **Farooq, W., Moon, M., Ryu, B.-G., Suh, W. I., Shrivastav, A., Park, M. S., Mishra, S. K., and Yang, J.-W.:** Effect of harvesting methods on the reusability of water for cultivation of *Chlorella vulgaris*, its lipid productivity and biodiesel quality, Algal Res., **8**, 1–7 (2015).
10. **Denis, C., Massé, A., Fleurence, J., and Jaouen, P.:** Concentration and pre-purification with ultrafiltration of a R-phycoerythrin solution extracted from macro-algae *Grateloupia turuturu*: process definition and up-scaling, Sep. Purif. Technol., **69**, 37–42 (2009).
11. **Qu, F., Yan, Z., Liu, W., Shao, S., Ren, X., Ren, N., Li, G., and Liang, H.:** Effects of manganese dioxides on the ultrafiltration membrane fouling by algal extracellular organic matter, Sep. Purif. Technol., **153**, 29–36 (2015).
12. **Qu, F., Liang, H., Tian, J., Yu, H., Chen, Z., and Li, G.:** Ultrafiltration (UF) membrane fouling caused by cyanobateria: fouling effects of cells and extracellular organics matter (EOM), Desalination, **293**, 30–37 (2012).
13. **Gao, W., Liang, H., Ma, J., Han, M., Chen, Z.-L., Han, Z.-S., and Li, G.-B.:** Membrane fouling control in ultrafiltration technology for drinking water production: a review, Desalination, **272**, 1–8 (2011).
14. **Zhang, X., Hu, Q., Sommerfeld, M., Puruhito, E., and Chen, Y.:** Harvesting algal biomass for biofuels using ultrafiltration membranes, Bioresour. Technol., **101**, 5297–5304 (2010).
15. **Babel, S. and Takizawa, S.:** Microfiltration membrane fouling and cake behavior during algal filtration, Desalination, **261**, 46–51 (2010).
16. **Al-Malack, M. H.:** 10-Treatment of petroleum refinery wastewater using crossflow and immersed membrane processes, Desalin. Water Treat., **51**, 6985–6993 (2013).
17. **Hung, M. T. and Liu, J. C.:** Microfiltration of microalgae in the presence of rigid particles, Sep. Purif. Technol., **198**, 10–15 (2018).
18. **Bilad, M. R., Mezohegyi, G., Declerck, P., and Vankelecom, I. F.:** Novel magnetically induced membrane vibration (MMV) for fouling control in membrane bioreactors, Water Res., **46**, 63–72 (2012).
19. **Bilad, M. R., Discart, V., Vandamme, D., Foubert, I., Muylaert, K., and Vankelecom, I. F.:** Harvesting microalgal biomass using a magnetically induced membrane vibration (MMV) system: filtration performance and energy consumption, Bioresour. Technol., **138**, 329–338 (2013).

20. **Genkin, G., Waite, T., Fane, A., and Chang, S.:** The effect of vibration and coagulant addition on the filtration performance of submerged hollow fibre membranes, J. Membr. Sci., **281**, 726–734 (2006).
21. **Hwang, K.-J. and Lin, S.-J.:** Filtration flux–shear stress–cake mass relationships in microalgae rotating-disk dynamic microfiltration, Chem. Eng. J., **244**, 429–437 (2014).
22. **Kim, K., Jung, J.-Y., Kwon, J.-H., and Yang, J.-W.:** Dynamic microfiltration with a perforated disk for effective harvesting of microalgae, J. Membr. Sci., **475**, 252–258 (2015).
23. **Zhao, F., Chu, H., Su, Y., Tan, X., Zhang, Y., Yang, L., and Zhou, X.:** Microalgae harvesting by an axial vibration membrane: the mechanism of mitigating membrane fouling, J. Membr. Sci., **508**, 127–135 (2016).
24. **Bartman, A. R., McFall, C. W., Christofides, P. D., and Cohen, Y.:** Model-predictive control of feed flow reversal in a reverse osmosis desalination process, J. Process Contr., **19**, 433–442 (2009).
25. **Uchymiak, M., Bartman, A. R., Daltrophe, N., Weissman, M., Gilron, J., Christofides, P. D., Kaiser, W. J., and Cohen, Y.:** Brackish water reverse osmosis (BWRO) operation in feed flow reversal mode using an ex situ scale observation detector (EXSOD), J. Membr. Sci., **341**, 60–66 (2009).
26. **Hargrove, S. C., Parthasarathy, H., and Ilias, S.:** Flux enhancement in cross-flow membrane filtration by flow reversal: a case study on ultrafiltration of BSA, Sep. Sci. Technol., **38**, 3133–3144 (2003).
27. **Chen, Y.-C.:** Immobilized microalga *Scenedesmus quadricauda* (Chlorophyta, Chlorococcales) for long-term storage and for application for water quality control in fish culture, Aquaculture, **195**, 71–80 (2001).
28. **Omar, H.:** Bioremoval of zinc ions by *Scenedesmus obliquus* and *Scenedesmus quadricauda* and its effect on growth and metabolism, Int. Biodeter. Biodegradation, **50**, 95–100 (2002).
29. **Ma, J., Lin, F., Zhang, R., Yu, W., and Lu, N.:** Differential sensitivity of two green algae, *Scenedesmus quadricauda* and *Chlorella vulgaris*, to 14 pesticide adjuvants, Ecotoxicol. Environ. Saf., **58**, 61–67 (2004).
30. **Awasthi, M. and Rai, L. C.:** Toxicity of nickel, zinc, and cadmium to nitrate uptake in free and immobilized cells of *Scenedesmus quadricauda*, Ecotoxicol. Environ. Saf., **61**, 268–272 (2005).
31. **Mata, T. M., Martins, A. A., and Caetano, N. S.:** Microalgae for biodiesel production and other applications: a review, Renew. Sustain. Energy Rev., **14**, 217–232 (2010).
32. **Kent, F. C., Adams, N. W. H., and Cadera, J.:** Immersed membrane filtration cycle with extended or tmp controlled cycle time. US Patent Application 20070256974 A1 (2007).
33. **Zhang, W., Shi, Z., Zhang, F., Liu, X., Jin, J., and Jiang, L.:** Superhydrophobic and superoleophilic PVDF membranes for effective separation of water-in-oil emulsions with high flux, Adv. Mater., **25**, 2071–2076 (2013).
34. **Zhang, W., Zhang, W., Zhang, X., Amendola, P., Hu, Q., and Chen, Y.:** Characterization of dissolved organic matters responsible for ultrafiltration membrane fouling in algal harvesting, Algal Res., **2**, 223–229 (2013).
35. **Zhang, X., Chen, Y., Konsowa, A. H., Zhu, X., and Crittenden, J. C.:** Evaluation of an innovative polyvinyl chloride (PVC) ultrafiltration membrane for wastewater treatment, Sep. Purif. Technol., **70**, 71–78 (2009).
36. **Schneider, C. A., Rasband, W. J., and Eliceiri, K. W.:** NIH Image to ImageJ: 25 years of image analysis, Nat. Med., **9**, 671–675 (2012).
37. **Zhang, X., Hewson, J. C., Amendola, P., Reynoso, M., Sommerfeld, M., Chen, Y., and Hu, Q.:** Critical evaluation and modeling of algal harvesting using dissolved air flotation, Biotechnol. Bioeng., **111**, 2477–2485 (2014).
38. **Fane, A. G., Beatson, P., and Li, H.:** Membrane fouling and its control in environmental applications, Water Sci. Technol., **41**, 303–308 (2000).
39. **Lobo, A., Cambiella, Á., Benito, J. M., Pazos, C., and Coca, J.:** Ultrafiltration of oil-in-water emulsions with ceramic membranes: influence of pH and cross-flow velocity, J. Membr. Sci., **278**, 328–334 (2006).
40. **Chiou, Y.-T., Hsieh, M.-L., and Yeh, H.-H.:** Effect of algal extracellular polymer substances on UF membrane fouling, Desalination, **250**, 648–652 (2010).
41. **Wu, X., Zhou, C., Li, K., Zhang, W., and Tao, Y.:** Probing the fouling process and mechanisms of submerged ceramic membrane ultrafiltration during algal harvesting under sub- and super-critical fluxes, Sep. Purif. Technol., **195**, 199–207 (2018).
42. **Monte, J., Sá, M., Galinha, C. F., Costa, L., Hoekstra, H., Brazinha, C., and Crespo, J. G.:** Harvesting of *Dunaliella salina* by membrane filtration at pilot scale, Sep. Purif. Technol., **190**, 252–260 (2018).
43. **Meng, F., Liao, B., Liang, S., Yang, F., Zhang, H., and Song, L.:** Morphological visualization, componential characterization and microbiological identification of membrane fouling in membrane bioreactors (MBRs), J. Membr. Sci., **361**, 1–14 (2010).
44. **Liu, J. X., Dong, B. Z., and Huang, W. W.:** Characteristics of fouled and chemically cleaned membrane, Adv. Mater. Res., **1073–1076**, 751–754 (2014).
45. **Wu, J., Le-Clech, P., Stuetz, R. M., Fane, A. G., and Chen, V.:** Effects of relaxation and backwashing conditions on fouling in membrane bioreactor, J. Membr. Sci., **324**, 26–32 (2008).
46. **Choi, H., Zhang, K., Dionysiou, D. D., Oerther, D. B., and Sorial, G. A.:** Influence of cross-flow velocity on membrane performance during filtration of biological suspension, J. Membr. Sci., **248**, 189–199 (2005).
47. **Liu, R., Huang, X., Sun, Y. F., and Qian, Y.:** Hydrodynamic effect on sludge accumulation over membrane surfaces in a submerged membrane bioreactor, Process Biochem., **39**, 157–163 (2003).